Chapter 2

The Design of a 360°-Switched-Beam-Base Station Antenna

Mohamed Aymen El Cafsi, Mourad Nedil,
Lotfi Osman and Ali Gharsallah

Additional information is available at the end of the chapter

http://dx.doi.org/10.5772/67522

Abstract

The concept of switched-beam antenna (SBA) systems covering an area of 360° for wireless base station applications is presented. First, a reconfigurable pattern antenna (RPA), which is composed of an omnidirectional slot-antenna array surrounded by an active cylindrical frequency selective surface (FSS), is studied. The behavior of FSS is controlled by PIN diodes which are able to divide the Azimuth plane into six sectors from one common source. Unfortunately for a sector antenna, a huge number of diodes are required which complicates the structure in terms of efficiency and complexity. However, a simple and an efficient SBA configuration based on a hexagonal Fabry-Pérot cavity leaky wave antenna (FPC LWA) arrays is proposed as a solution for RPA problems. A sector-directive beam is generated from a simple patch antenna embedded inside a resonant Fabry-Pérot cavity with specific dimensions which have an influence on beamwidth and radiation efficiency. To increase more sectorization level and channel's capacity, the proposed sector in FPC LWA arrays can be divided into three subsectors by using an active high-impedance surface (HIS). As a conclusion, SBA based on FPC LWA is the most suitable solution for future wireless communications.

Keywords: switched-beam antenna, base station, reconfigurable pattern antenna, frequency-selective surface, Fabry-Pérot cavity leaky wave antenna

1. Introduction

Wireless communications are evolving to offer new generations of services such as video, satellite broadcasting, Internet, and mobile networks, which require high throughput to transmit multimedia signals with a good reliability [1]. In fact, these requirements force

the improvement of the immunity of base station in front of many constraints such as multipath fading and interferences created between wireless networks due to an omnidirectional radiation pattern [2].

Beamforming is seen as a solution for the problems cited previously to ensure a high quality of service (QoS) and increased channel capacity using smart antenna systems [3].

Basically, a smart antenna system is based on the theory of phased antenna arrays wherein the differential phase between adjacent antennas permits the scan of radiation pattern. Depending on their architectures, these systems are divided into two categories based on transmit strategy: adaptive antennas and switched-beam antenna (SBA) [4].

Adaptive antennas are able to adapt their radiation patterns by exploiting the wireless radio channel at both transmitter and receiver sides with high precision using digital signal processing. Moreover, these adaptive systems have the ability to distinguish between user signal and interferences and also to steer the main beam in the desired direction with insertion zeros, thereby increasing the signal-to-interferences ratio [2].

However, the physical implementation of this system is very complex and expensive and requires high-power consumption and a longer time period to compute the current weight's values (amplitude and phase) for each antenna which is not suitable for high data rate communications [4].

On the other side, the SBA generates multiple fixed beams in a specific area. The behavior of these systems consists in the detection of the user's position by measuring signal strength, selects one of the predefined fixed beams and switches from one beam to another when the user moves [4].

In general, switching operation is assured by a fixed beamforming network, such as Blass matrix [5], Rotman lens [6, 7], and Butler matrix [4], connected to a linear antenna array. When interference and useful signal are both located in the same beam, the SBA system is disabled to resolve this scenario compared to the adaptive antennas [8]. Thus, the SBA is less costly, but its complexity and losses increase when the number of beams is increased.

In addition, these two classical smart antenna systems do not provide 360° of coverage due to the printed circuit broad (PCB) technique used on the design of antenna which radiates above the ground plane of the structure allowing only half-plane coverage. Moreover, if the antenna element has an omnidirectional radiation pattern, such as monopole, the directivity will be divided into two opposed directions that are decreasing, which causes the radiated energy.

Two SBA configurations, allowing 360° coverage, are presented in this chapter, which is organized as follows. After the introduction, an RPA is presented using as a technique to create SBA, which is obtained from an omnidirectional source surrounded by an active FSS, wherein active elements are mounted on its surface. However, this type of configuration requires a huge number of switchers such as PIN diodes that complicate the structure. To overcome the use of the PIN diodes and achieve directive beam from one low-gain

source, Section 3 presents a simple and an efficient hexagonal SBA configuration based on Fabry-Pérot cavity leaky wave antenna (FPC LWA) arrays. Finally, the last section concludes the chapter.

2. Reconfigurable switched-beam antenna using an active cylindrical frequency-selective surface

2.1. FSS unit cell

FSS is an artificial electromagnetic band gap (EBG) metamaterial periodic structures which has the ability to control the propagation of electromagnetic waves, as spatial filter, in a specific frequency band [4, 9].

This behavior can be used as a beamforming technique for covering an area of 360° and creating a smart antenna. The proposed periodic unit-cell structure presented in **Figure 1** is composed of a discontinuous metal strip printed on a flexible substrate where a PIN diode is inserted in the discontinuity [9].

According to the PIN diode state, the strip has a reconfigurable transmission/reflection coefficient [10]. When the diode is turned ON, it is equivalent to a resistor and acts as a reflector. While for OFF state, the diode is equivalent to parallel RC circuit allowing the strip to be transparent to the electric field of a transverse electric (TE) plane wave which is parallel to it [9, 10].

Figure 2 illustrates the reflection/transmission coefficients of the proposed FSS unit cell.

A high reflection coefficient *R* is obtained for the ON state, whereas for the OFF state, a high transmission coefficient *T* is achieved.

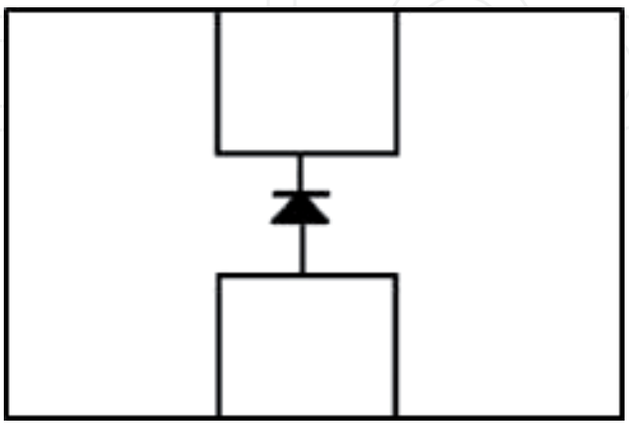

Figure 1. FSS unit cell.

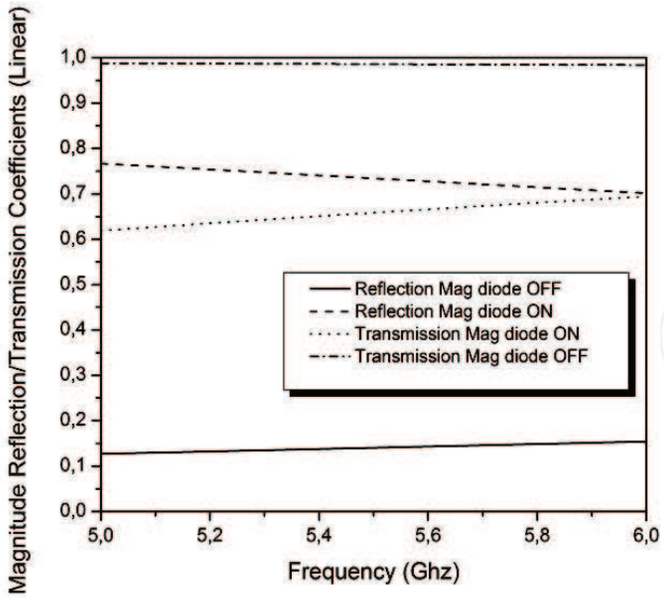

Figure 2. Magnitude of reflection/transmission coefficient of FSS unit cell.

Indeed, *R* and *T* are inversely proportional to the ON-state resistance and the OFF-state capacitance values, respectively [10].

So, the diode should have a low resistance's value in ON state and a low capacitance's value in OFF state. For the proposed design, the PIN diode GMP-4201 from MicroSemi is used and modeled with the ON-state resistor of R_{ON} = 2.3 Ω and, in the OFF-state, with parallel RC circuit with R_{OFF} = 30 KΩ and C_{OFF} = 0.18 pF [10]. The surface of the gap should be equal to the diode's dimensions.

2.2. Reconfigurable pattern antenna

In fact, RPA is achieved by placing an omnidirectional antenna in the center of the active cylindrical FSS. A sector notion is defined in this design by dividing the cylinder into two semi-cylinders. The first semi-cylinder is activated by turning its PIN diodes "ON" and behaves as a parabolic reflector which defines the directivity of radiation pattern. However, the other diodes are turned OFF and the second semicylinder will be transparent to the electromagnetic waves allowing radiation [10].

So, by controlling PIN diode states, a dynamic FPC antenna is obtained which is able to scan all azimuth planes from an omnidirectional source.

2.2.1. Omnidirectional slot-array antenna

If the source used is a simple dipole, the system will suffer from a low directivity due to the small aperture surface of FSS [11]. To enhance the directivity, authors in [10] have used a dipole array wherein pipes are used between two successive dipoles to ensure impedance

http://dx.doi.org/10.5772/67522

matching and in-phase excitation of the array. Again, the use of pipes complicates the system in terms of adaptation.

To overcome problems cited above, a high-gain omnidirectional radiation pattern can be obtained from a printed slot array which is fed by a strip line embedded in sandwich between two substrates with the same thickness as shown in **Figure 3**. The radiation phenomenon is done from the two ground planes situated at the top and bottom of the structure [9].

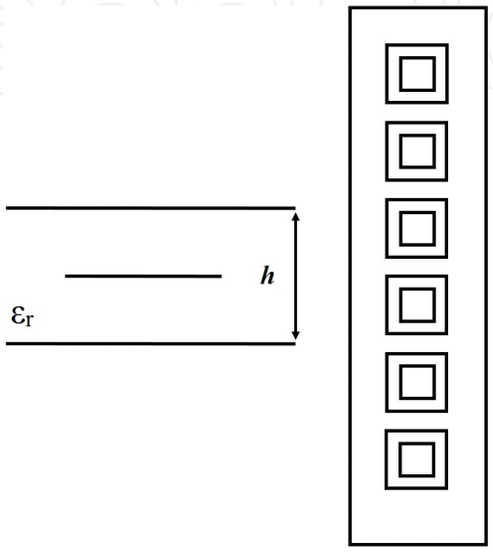

Figure 3. Omnidirectional slot-antenna array.

Return loss and radiation pattern in H- and E-planes are shown in **Figures 4** and **5**, respectively. The structure operates at 5.8-GHz central frequency of Industrial Scientific Medical (ISM) band with 1.72% of the bandwidth.

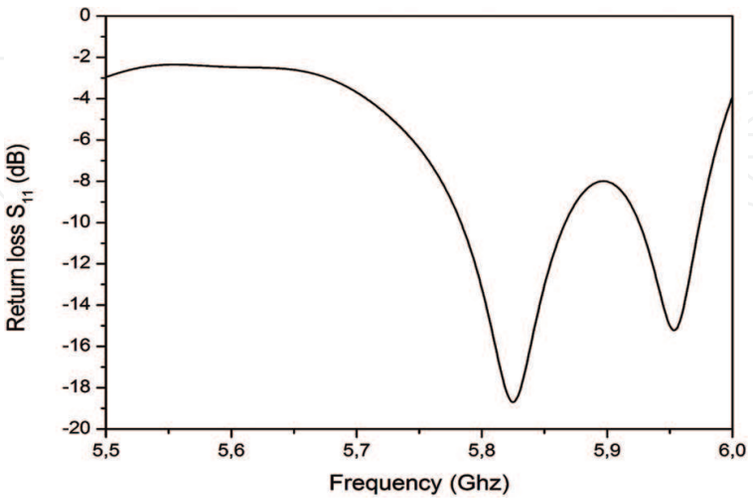

Figure 4. Return loss of slot-antenna array.

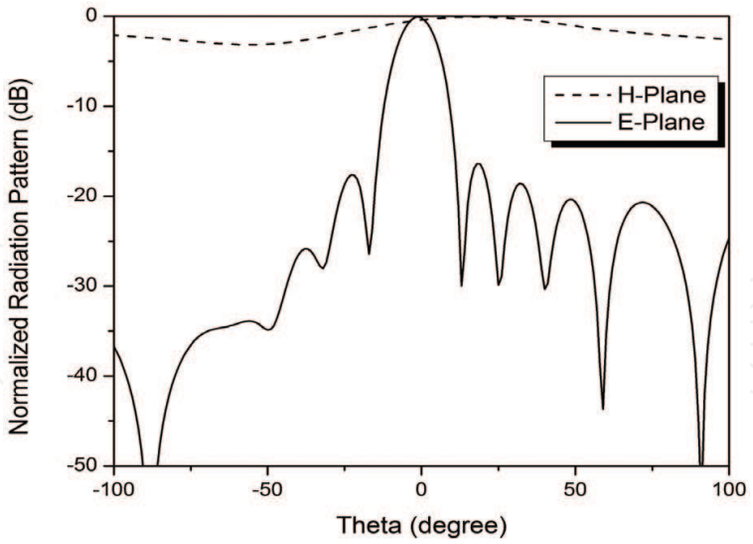

Figure 5. Radiation pattern in H- and E-planes.

Due to its constant values in all directions and according to **Figure 5**, the reconfigurable radiation pattern is located in H-plane and will be used to divide the azimuth plane in many fixed sectors.

2.2.2. Switched-beam antenna system

The whole reconfigurable antenna system, which is composed of the slot-antenna arrays surrounded by the active conformal FSS, is given in **Figure 6**.

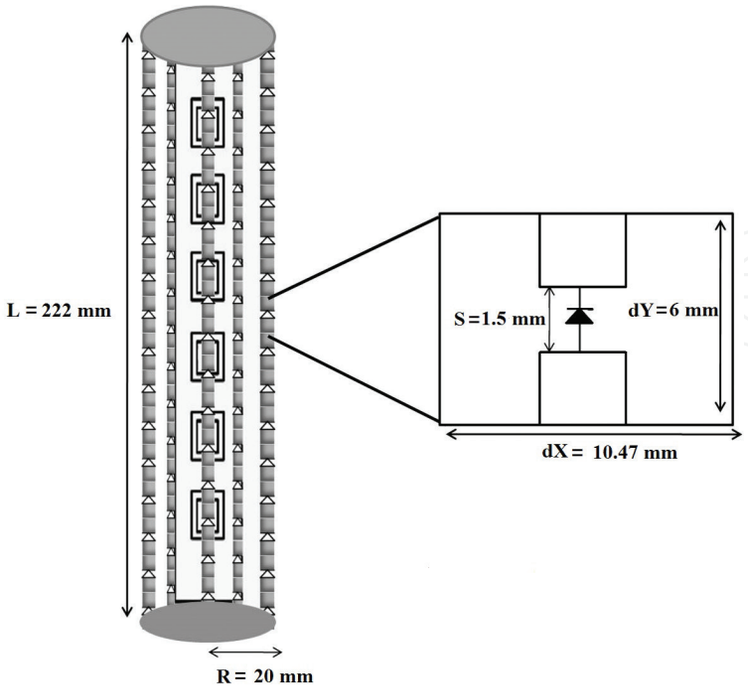

Figure 6. Reconfigurable pattern antenna.

http://dx.doi.org/10.5772/67522

A recent study reported in [12] demonstrates that six-sector deployments increase the channel capacity by 70–80% compared to traditional three sector sites. Therefore, FSS parameters, which are the number of strips N, the width of unit cell $D_{x,}$ and the radius R, are studied to satisfy this requirement using the following equations [10]:

$$N = \frac{360}{P_\theta} \tag{1}$$

$$D_x = R \,.\, P_\theta \cdot \frac{\pi}{180} \tag{2}$$

where P_θ is the period angular and, in this case, is equal to 30°.

The activated strip number, whose PIN diodes are turned ON, has an influence on the H-plane beamwidth and equals 4, in the proposed design, to achieve a symmetrical half beamwidth of 70° as shown in **Figure 7**.

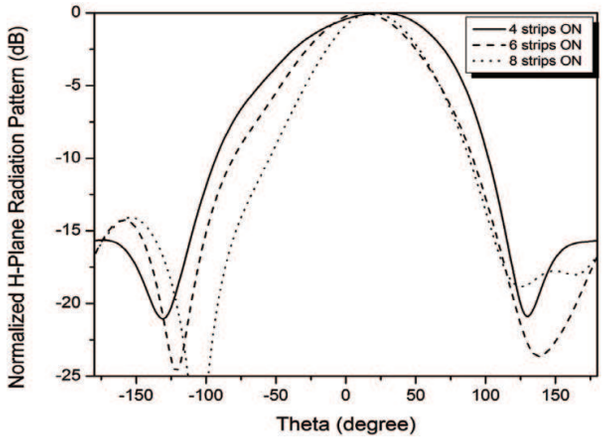

Figure 7. Effect of strips in ON state on H-plane radiation pattern.

The effect of FSS radius on radiation pattern is presented in **Figure 8** where the optimum value found is close to the half wavelength of the operating frequency in free space.

Figure 9 illustrates six switched beams covering all azimuth planes.

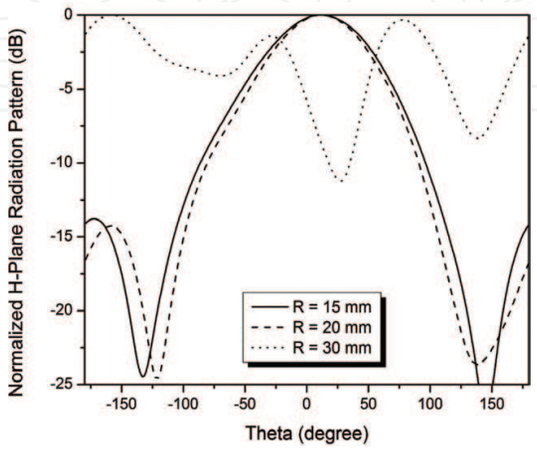

Figure 8. Effect of FSS cylinder radius on H-plane radiation pattern.

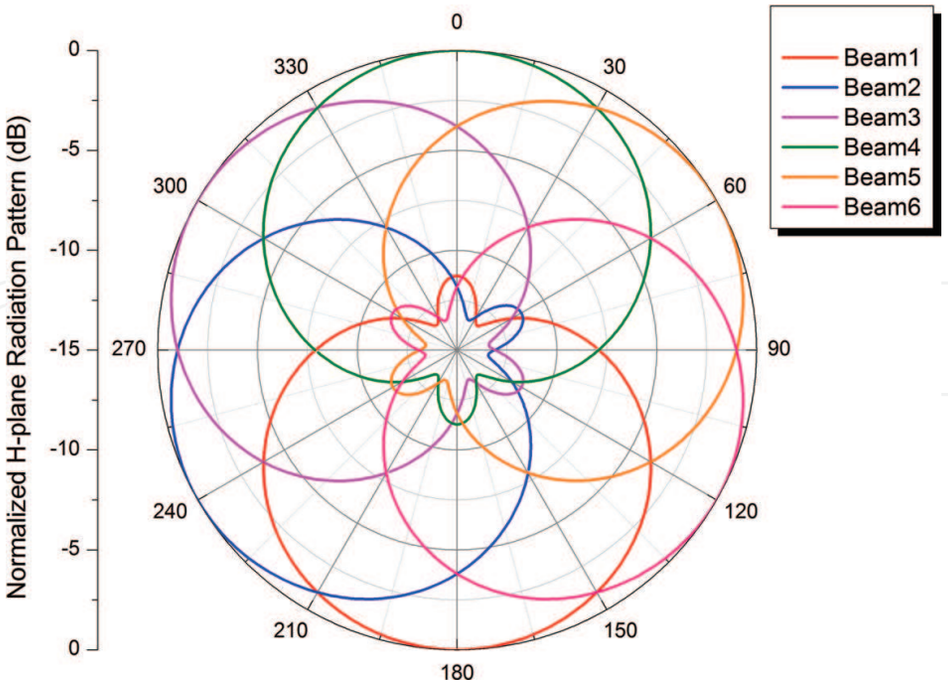

Figure 9. Switched-beam antenna.

With these optimum parameters of FSS, a directional sector antenna is achieved offering 12 dBi of directivity with a wide beam in H-plane and a narrow beam in E-plane. The proposed antenna is surrounded by 12 strips along the antenna length and each strip requires 36 PIN diodes. As a result, a huge number of active elements are required, which decreases the radiation efficiency and increases the cost and complexity of the system.

3. An efficient hexagonal switched-beam antenna structure based on Fabry-Pérot cavity leaky wave antenna

SBA system based on a planar FPC LWA is proposed, in this section, as a solution to avoid the use of PIN diode on an RPA system.

In general, a planar resonant FPC is composed from an x-directed horizontal electric dipole (HED) backed with a ground plane and PRS superstrate placed on top of the structure [13, 14] as shown in **Figure 10**.

This type of structure is seen as a leaky parallel waveguide or two-dimensional (2D) leaky wave antenna which is able to produce a pencil beam at broadside under a specific condition [14, 15]

$$\frac{h}{\lambda_0} = \frac{0.5}{\sqrt{\varepsilon_r - \sin^2(\theta_i)}} = \frac{0.5}{\cos(\theta_i)} \tag{3}$$

where h is the distance between the ground plane and PRS screen, λ_0 is the free space wavelength, ε_r permittivity of the medium of propagation, and θ_i is the incident wave angle.

http://dx.doi.org/10.5772/67522

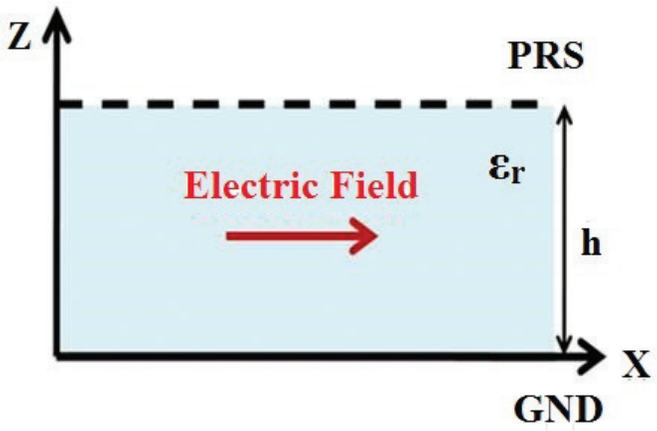

Figure 10. Two-dimensional leaky wave antenna.

For air-filled cavity ($\varepsilon_r = 1$) and at broadside ($\theta_i = 0°$), the incident wave propagation has a normal angle to structure providing a distance h equal to half wavelength of the operating frequency in free space.

In this proposed design, a simple patch antenna, printed on the Rogers RT5880 substrate (permittivity $\varepsilon_r = 2.2$ and thickness $h = 1.575$ mm), is used as HED and resonates at the frequency 5.8 GHz. However, PRS is made from an inductive metal strip grating (MSG) [16] screen printed on Rogers RT6010 superstrate (permittivity $\varepsilon_r = 10.2$ and thickness $t = 2.5$ mm) with the following parameters: width of strips $w = 5$ mm and period of strips $P = 7$ mm) [4, 17].

The proposed FPC LWA is presented in **Figure 11**.

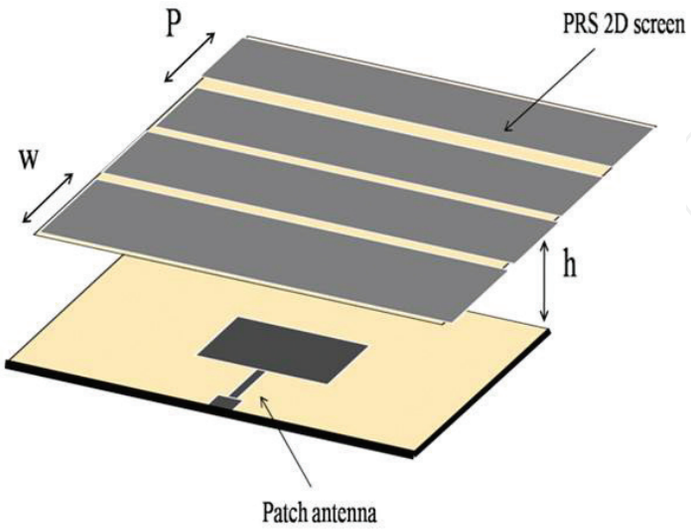

Figure 11. Fabry-Pérot cavity leaky wave antenna.

3.1. Azimuth division approach

Our sectorization approach consists of dividing the azimuth plane in N sectors where N is defined according to an angle ϕ formed between two successive cavities FPC LWA forming a specific shape [4, 17].

By fixing the size on y-direction, a superstrate portion ΔL is added in two edges to interconnect the two adjacent PRS screens and, in this case, we talk about one-dimension (1D) FPC LWA which enhances the gain of the patch antenna by a factor about 3 dB [4].

Furthermore, PRS length controls the attenuation constant α of the propagation constant k inside cavity which has an influence on the radiation efficiency [18, 19].

The leakage rate or attenuation coefficient α and radiation efficiency (η_{RA}) are obtained using the following formulas, respectively [20]:

$$\alpha = \frac{S_{\mathrm{SLL}}}{8.686L} \tag{4}$$

$$\eta_{RA}(\%) = 1 - \exp\left[-2\alpha\left(\frac{L}{2} + \Delta L\right)\right] \tag{5}$$

where S_{SLL} is the side-lobe level (in dB) and L is the total length of PRS along x-direction.

The effect of sector number on antenna radiation efficiency is summarized in **Table 1** and **Figure 12**.

Angle (in degree)	ΔL (in mm)	Attenuation coefficient α (in m^{-1})	Directivity (in dBi)	Number of sectors	Side-lobe levels (in dB)	Total length of PRS (in mm)	Radiation efficiency (%)
10	2.5	0.021	10.52	36	−12.2	65	74.46
20	5	0.02	10.5	18	−12.2	70	75.34
30	7.5	0.018	10.53	12	−12.2	75	74.07
40	10	0.0175	10.74	9	−12.5	80	75.34
60	16	0.0211	11.39	6	−16.2	92	85.64
90	28	0.013	10.55	4	−13.3	116	77.86
120	46	0.0123	10.3	3	−16.2	152	84.585

Table 1. The effect of sector number on antenna radiation efficiency.

The optimal radiation efficiency is achieved for six and three sectors and its values are close to the optimum radiation efficiency (87%) predicted in [20].

However, a directivity of 11.39 dBi is achieved for six sectors compared with 10.3 dBi for three sectors despite the large length of PRS [4]. This observation can be explained by the existence of an optimal size for the cavity which limits radiation efficiency.

The whole SBA FPC-LWA system is illustrated in **Figure 13**. It is composed of the hexagonal FPC LWA arrays connected to a Single Pole 6 Throws (SP6T) RF switcher [21] which switches the common input power between six outputs.

http://dx.doi.org/10.5772/67522

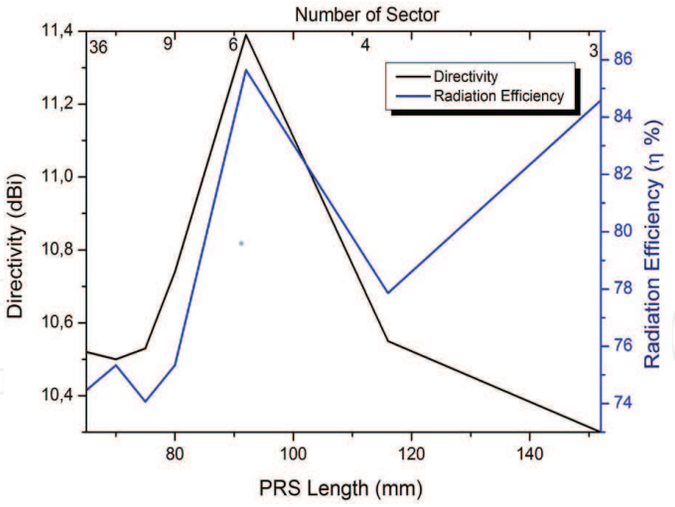

Figure 12. Radiation efficiency and directivity versus PRS length and number of sectors.

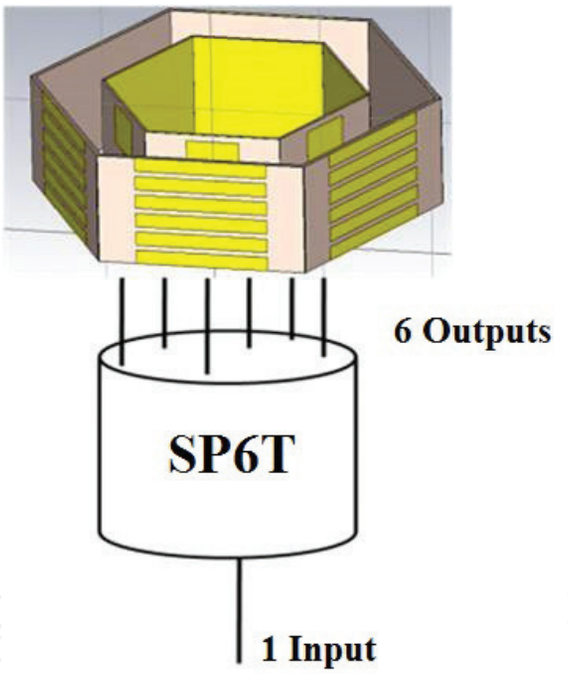

Figure 13. The proposed hexagonal switched-beam antenna system.

The photograph of fabricated prototype is shown in **Figure 14**.

The simulation and experimental results of return loss are shown in **Figure 15**. From these curves, it can be concluded that a bandwidth of 100 MHz is obtained for a return loss below 10 dB. Due to the repetitive recurrence of the structure, all coverage directions have the same bandwidth which represents 1.46% of the total bandwidth at the central frequency 5.8 GHz of ISM band.

It can be seen also that measured result is shifted on the left from the simulation caused by the height of cavity which exceeds slightly a half wavelength found by Eq. (3).

Figure 14. Fabricated prototype.

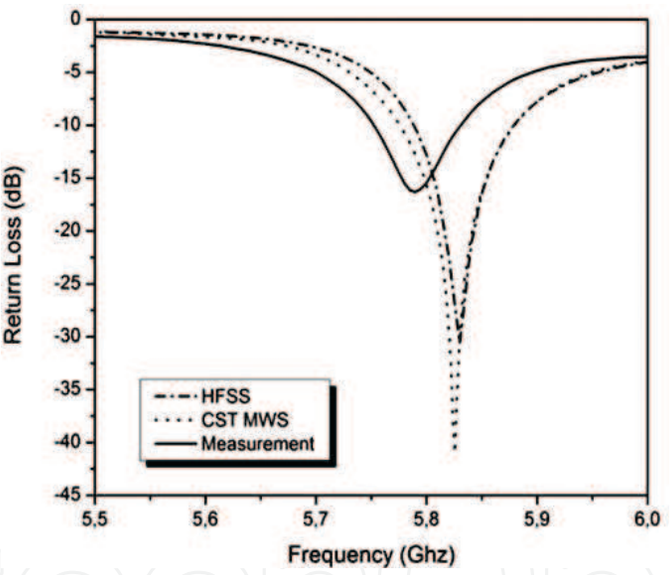

Figure 15. Return loss.

Simulated and experimental radiation patterns in the azimuth plane or E-plane are shown in **Figure 16** wherein a good agreement is carried out. A sector is defined by 3-dB beam width around 30°,which is the half value found in RPA [4], and according to [22], this beamwidth value allows to decrease the overlap between beams to 9 dB compared to 3 dB (the case of beamwidth of 60°) increasing thus signal-to-noise ratio (SNR).

The activate radiation pattern has a back-lobe level and a side lobe level of 15 dB. Some beams, in measurement, have high SLL which can be explained by the imperfect interconnection between two successive FPC LWA introducing parasite radiations.

http://dx.doi.org/10.5772/67522

It is important to see how the six beams cover all azimuth planes without any crossover between adjacent beams.

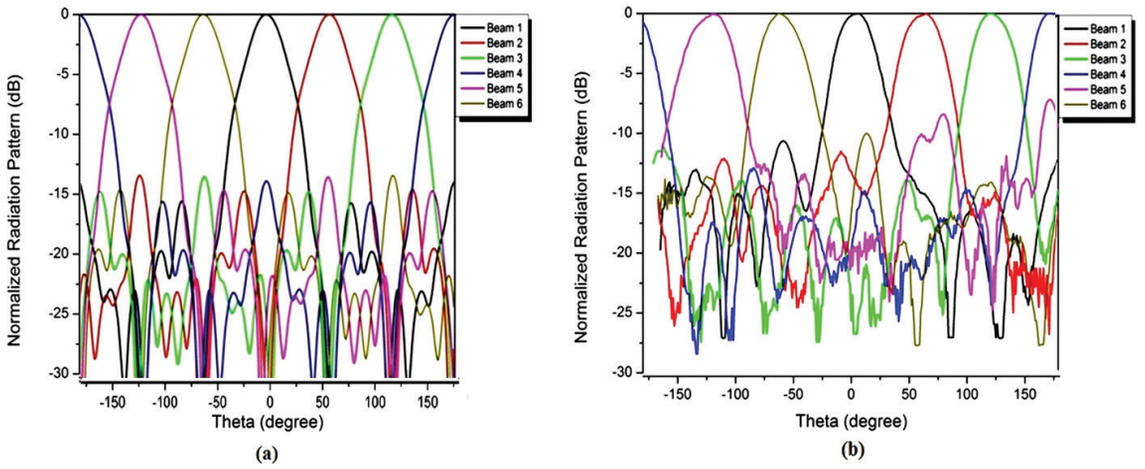

Figure 16. E-plane radiation pattern: (a) simulated and (b) measured.

Figure 17 presents the results of gain in the azimuth plane between 5.6 and 6 GHz found by measurement and simulation using two full-wave analyses Ansoft HFSS [23] and CST Microwave studio [24].

We noted an intersection between the measured value and the simulated one found by HFSS. This observation confirms our previous study which proposed that FPC LWA has a high radiation efficiency as presented in Section 3.1.

As result, a gain around 10 dBi is obtained for both simulation and measurement. However, a simulated value of CST Microwave studio is greater than HFSS by 1 dB, which can be explained by the different methods used in the simulation process.

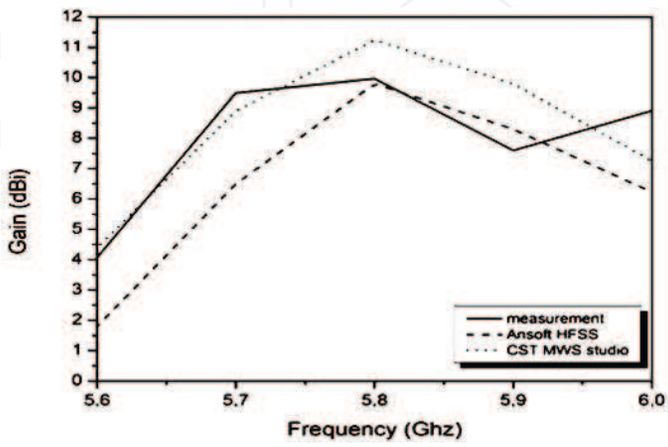

Figure 17. Simulated and measured gain.

3.1.1. Sector division

Dividing the sector into subsectors or small cells further enhances the channel's capacity by increasing the sectorization level. As an example, an active high-impedance surface (HIS) based on electromagnetic band gap mushroom-like structure, located on the ground plane of 50 ohms fed coaxial patch antenna [3], can be used as beamforming technique to scan the beam inside sector as shown in **Figure 18**.

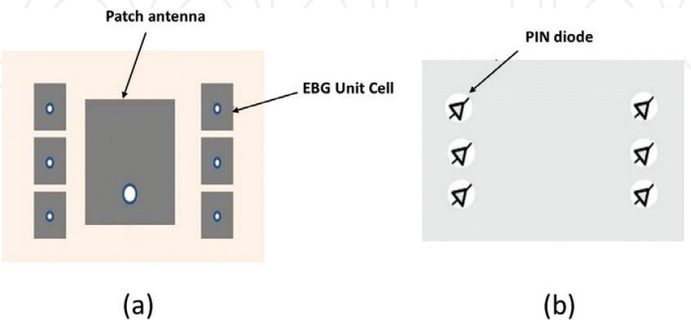

Figure 18. Reconfigurable pattern antenna using HIS structure: (a) top view and (b) bottom view.

Six PIN diodes are used as a switcher to control the surface-wave propagation according to the equation [3]

$$\frac{\beta}{k_0} = \sin(\theta) \tag{6}$$

where β is phase coefficient of complex constant propagation k, k_0 is the free space wavenumber, and θ is the steered angle of the radiation pattern.

As seen previously in Section 2, the HIS ground plane is divided in two parts: one part acts as a reflector for TE surface wave by activating the corresponding PIN diodes. While other PIN

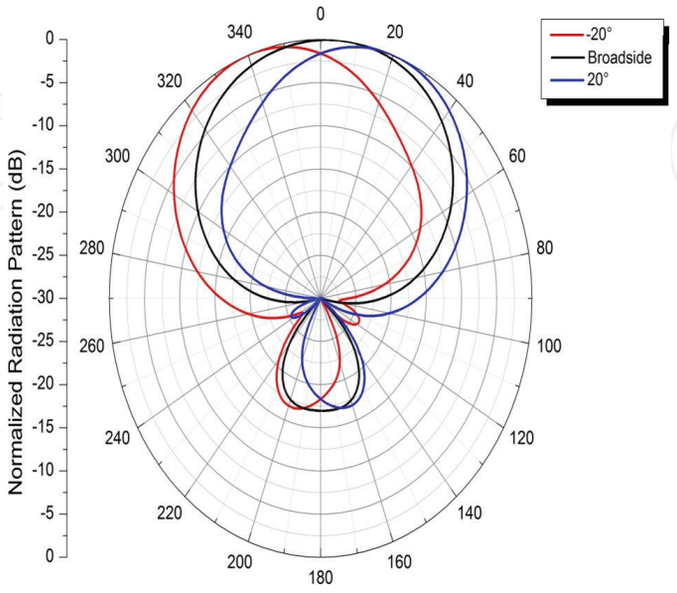

Figure 19. Small-cell normalized Azimuthal radiation patterns.

http://dx.doi.org/10.5772/67522

diodes are turned OFF, allowing the propagation of TM surface waves which radiate with patches printed on top of the substrate.

According to **Figure 19**, three steered beams inside a sector at −20°, 0°, and 20° are achieved, respectively.

By replacing the PRS of the hexagonal FPC LWA by the proposed active HIS, the whole system divides the Azimuth plane in 18 sectors, according to **Figure 20**, in simple ways using few PIN diodes [3].

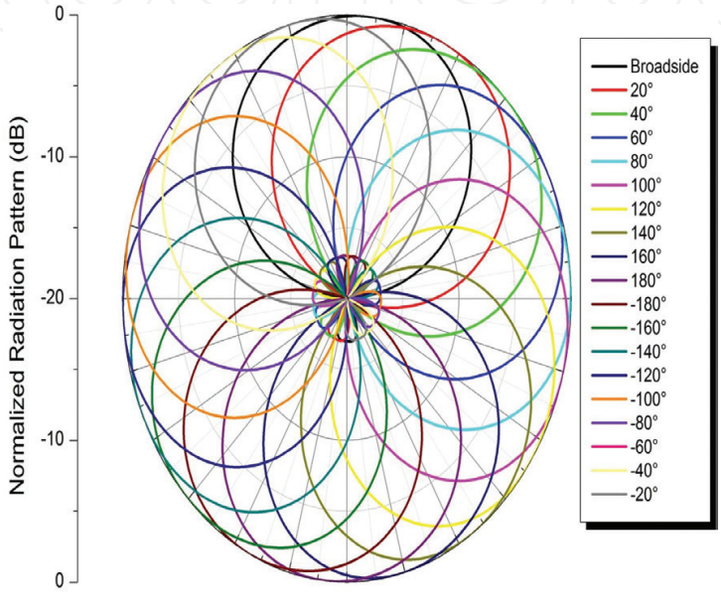

Figure 20. Eighteen beams covering azimuth plane.

4. Conclusion

SBA systems based on periodic metal structures have been presented in this chapter showing their ability in 360° of azimuthal coverage for base station applications. First, RPA has been studied which is composed of a linear slot-antenna array surrounded by an active FSS. In this design, PIN diodes are used as a switcher to control FSS response, giving an agility to omnidirectional radiation pattern and create SBA which divides the azimuth plane in six sectors. However, the major drawback of this system consists of a large number of active elements used which introduces losses and complicates the system's architecture.

For that, a hexagonal FPC LWA array has been proposed as solution to overcome problems related to PIN diodes. A high gain and good radiation efficiency are obtained from patch antenna, located inside a planar FPC, to avoid the use of antenna arrays with their complex feeding networks. An external SP6T RF switcher is required to be connected to FPC LWA arrays to switch the beam from a sector to another.

To increase more sectorization level, a reconfigurable HIS ground plane is proposed as a beamforming technique to divide the sector in three small cells. As a result, 18 beams are

achieved covering all azimuth planes. The proposed SBA structure, based on FPC LWA, is the most suitable for future wireless base station applications due to its simplicity.

Author details

Mohamed Aymen El Cafsi[1]*, Mourad Nedil[2], Lotfi Osman[1] and Ali Gharsallah[1]

*Address all correspondence to: aymenelcafsi@gmail.com

1 Faculty of Sciences of Tunis, University of Tunis El Manar, UR13ES37 Unit of Research in High Frequency Electronics Circuits and Systems, Tunis, Tunisia

2 University of Quebec in Abitibi-Témiscamingue, Engineering School, Québec, Canada

References

[1] Habib M.A., Jazi M.N., Djaiz A., Nedil M., Denidni T.A. Switched-beam antenna based on EBG periodic. In: IEEE, editor. IEEE MTT-S International Microwave Symposium Digest; 7–12 June 2009; Boston. IEEE; 2009. DOI: 10.1109/MWSYM.2009.5165821

[2] Nedil M., Denidni T.A.,Talbi L. Novel butler matrix using CPW multilayer technology. IEEE Transactions on Microwave Theory and Techniques. 2006;**54**(1):499–507. DOI: 10.1109/TMTT.2005.860490

[3] El Cafsi M.A., Nedil M., Osman L., Gharsallah A. High sectorization switched beams for WLAN applications. In: IEEE International Symposium on Antennas and Propagation (APSURSI); 26 June–1 July; Puerto Rico. IEEE; 2016. pp. 2161–2162. DOI: 10.1109/APS.2016.7696787

[4] El Cafsi M.A., Nedil M., Osman L., Gharsallah A. An efficient hexagonal switched beam antenna structure based on Fabry-Pérot cavity leaky-wave antenna. International Journal of Electronics. 2015;**102**(11):1789–1803. DOI: http://dx.doi.org/10.1080/00207217.2014.996782

[5] Mosca S., Bilotti F., Toscano A., Vegni L. A novel design method for Blass matrix beam-forming networks. IEEE Transactions on Antennas and Propagation. 2002;**50**(2):225–232. DOI: 10.1109/8.997999

[6] Rotman W., Turner R.F. Wide-angle microwave lens for line source applications. IEEE Transactions on Antennas and Propagation. 1963;**11**(6):623–632. DOI: 10.1109/TAP.1963.1138114

[7] Christie S., Cahill R., Buchanan B., Fusco V.F., Mutchell N., Munro Y.V., Maxwell-Cox G. Rotman lens-based retro directive array. IEEE Transactions on Antennas and Propagation. 2012;**60**(3):1343–1351. DOI: 10.1109/TAP.2011.2180347

[8] Huang Y. Smart antenna systems for WiMAX radio technology. In: WIMAX New Developments. Rijeka: InTech; 2009. pp. 201–212. DOI: 10.5772/8269

[9] El Cafsi M.A., Nedil M., Osman L., Gharsallah A. A reconfigurable switched beam antenna using active cylindrical frequency selective surface. In: 26th IEEE Canadian Conference Of Electrical And Computer Engineering (CCECE); May 5–8; Regina, Canada. IEEE; 2013. pp. 1–4. DOI: 10.13140/RG.2.1.5094.3448

[10] Edalati A., Denidni T.A. High-gain reconfigurable sectoral antenna using an active cylindrical FSS structure. IEEE Transactions on Antennas and Propagation. 2011;**59**(7):2464–2472. DOI: 10.1109/TAP.2011.2152327

[11] Bouslama M., Traii M., Denidni T.A., Gharsallah A. Beam-switching antenna with a new reconfigurable frequency selective surface. IEEE Antennas and Wireless Propagation Letters. 2015;**15**:1159–1162. DOI: 10.1109/LAWP.2015.2497357

[12] COMMSCOPE. Six sector Solution [Internet]. 2013.Available from: http://www.commscope.com/Solutions/Six-Sector-Turnkey-Solution/

[13] Burghignoli P., Lovat G., Capolino F., Jackson D.R., Wilton D.R. High polarized, directive radiation from a Fabry-Pérot cavity leaky-wave antenna based on a metal strip grating. IEEE Transactions on Antennas and Propagation. 2010;**58**(12):3873–3883. DOI: 10.1109/TAP.2010.2078441

[14] Jackson D.R., Burghignoli P., Lovat G., Capolino F., Ji C., Wilton D.R., Oliner A.A. The fundamental physics of directive beaming at microwave and optical frequencies and the role of leaky waves. Proceeding of the IEEE. 2011;**99**(10):1780–1805. DOI: 10.1109/JPROC.2010.2103530

[15] Zhao T., Jackson D.R., Williams J.T., Oliner A.A. General formulas for 2-D leaky wave antennas. IEEE Transactions on Antennas and Propagation. 2005;**53**(11):3525–3533. DOI: 10.1109/TAP.2005.856315

[16] Lovat G., Burghignoli P., Capolino F., Jackson D.R., Wilton D.R. High gain omnidirectional radiations patterns from a metal strip grating leaky wave. In: IEEE International Symposium Antennas and Propagation Society; 9–15 June; Hawaii. IEEE; 2007. pp. 5797–5800. DOI :10.1109/APS.2007.4396869.

[17] El Cafsi M.A., Nedil M., Osman L., Gharsallah A. 1D switched beam Fabry-Pérot leaky wave antenna. In: IEEE Antennas and Propagation Society International Symposium (APSURSI); 2014; Memphis. IEEE; 2014. pp. 1798–1799. DOI: 10.1109/APS.2014.6905225

[18] Garcia-Vigueras M., DeLara-Guarch P., Gomez-Tomero J.L., Guzman-Quiros R., Goussetis G. Efficiently illuminated broadside-directed 1D and 2D tapered Fabry-Pérot leaky-wave antenna. In: 6th European Conference on Antenna and Propagation (EUCAP);2012; 26–30 March; Prague. IEEE; 2012. pp. 247–251. DOI: 10.1109/EuCAP.2012.6206359

[19] Gardelli R., Albani M., Capolino F. Array thinning by using antennas in a Fabry-Pérot cavity for gain enhancement. IEEE Transactions on Antennas and Propagation. 2006;**54**(7):1979–1990. DOI: 10.1109/TAP.2006.877172

[20] Komanduri V.R., Jackson D.R., Long S.A. Radiation characteristics of finite-length 1D-uniform leaky wave antennas radiating at broadside. In: IEEE International Symposium Antennas and Propagation Society; 11–17 July; Toronto. IEEE; 2010. DOI: 10.1109/APS.2010.5560977

[21] Jaewoo L., Chan Han J., Sungweon K., Choi C.A. A low-loss single-pole six throw switch based on compact RF MEMS switches. IEEE Transactions on Microwave Theory and Techniques. 2005;**53**(11):3335–3344. DOI: 10.1109/TMTT.2005.855746

[22] COMMSCOPE. Twin beam technology adds immediate capacity without additional antennas [Internet]. May 2013. Available from: http://www.commscope.com/Docs/Six-Sector_Twin_Beam_WP-106683.pdf

[23] Ansoft HFSS. High Frequency Electromagnetic Field Simulation [Internet]. Available from: http://www.ansys.com/Products/Electronics/ANSYS-HFSS

[24] CST Microwave Studio. CST MICROWAVE STUDIO [Internet]. Available from: https://www.cst.com/products/cstmws